

Mathematical model for steady state current at PPO-modified micro-cylinder biosensors

Kodhandapani Venugopal¹, Alagu Eswari², Lakshmanan Rajendran^{2*}

¹Department of Mathematics, J.J College of Engineering and Technology, Tiruchirappali, India;

²Department of Mathematics, The Madura College, Madurai, India.

Email: *raj_sms@rediffmail.com

Received 1 July 2011; revised 18 July 2011; accepted 3 August 2011.

ABSTRACT

A Mathematical model for a modified micro-cylinder electrode in which polyphenol oxidase (PPO) occurs for all values of the concentration of catechol and *o*-quinone is analysed. This model is based on system of reaction-diffusion equations containing a non-linear term related to Michaelis Menten kinetics of the enzymatic reaction. Here a new analytical technique Homotopy Perturbation Method is used to solve the system of non-linear differential equations that describe the diffusion coupled with a Michaelis-Menten kinetics law. Here we report an analytical expressions pertaining to the concentration of catechol and *o*-quinone and corresponding current in terms of dimensionless reaction-diffusion parameters in closed form. An excellent agreement with available limiting case is noticed.

Keywords: Non-Linear Reaction/Diffusion Equation; Biosensors; Polymer-Modified Micro-Cylinder Electrode; Polyphenol Oxidase; Homotopy Perturbation Method

1. INTRODUCTION

Microelectrodes are increasingly being used in biosensors [1-3]. This is due to factors such as fast response times, high signal: noise ratios and the ability to operate in low conductivity media, sub-micro volume and in vivo [4]. The most commonly used microelectrode in bio-sensor is microcylinder such as carbon fibres. This is because they are cheap, readily available, their form is suited to implantation [5] and because much is known about their surface characteristics [6].

Immobilization of enzymes is used in biosensors to detect the concentration of a specific analyte as a result of the biological recognition between the analyte and the immobilized enzyme. Enzymes have been immobilized

at carbon fibres by many methods. Among all the methods, layer-by-layer (LbL) self assembly process is a simple technique which may be applied to a wide range of enzymes and that it is one of the few immobilization procedures which allows control over the amount and spatial distribution of the enzyme [7]. This property is important both for constructing and modeling studies of biosensors. The layer-by-layer process was first introduced by Decher and Hong [7]. This method has been applied to planar electrodes of Au [8,9], carbon electrodes [10] and polystyrene latex [11-15].

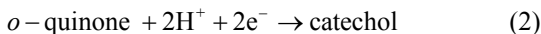
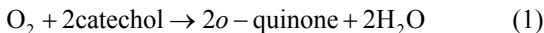
To analyse the performance of biosensors of any kind, it would be useful to have a mathematical model of the electrode response. Theoretical models of enzyme electrodes give information about the mechanism and kinetics operating in the biosensor. Unlike experimental investigations of biosensors, where changing one parameter inevitably alters others, the influence of individual variables can be assessed in an idealized way. Thus, the information gained from modeling can be useful in sensor design, optimization and prediction of the electrodes response.

Recently Rijiravanich *et al.* [16] obtained the steady state concentration profile of *o*-quinone and dimensionless sensor response j for the limiting cases of low substrate concentrations. To the best of our knowledge, no rigorous analytical solutions for the steady state concentrations for micro-cylinder biosensors for all values of the parameters have been published. In this communication, we have derived the new and simple analytical solutions of the concentration and the current for all values of parameters using the Homotopy Perturbation Method

2. MATHEMATICAL FORMULATION OF THE PROBLEM AND ANALYSIS

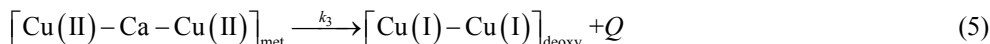
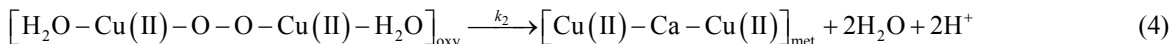
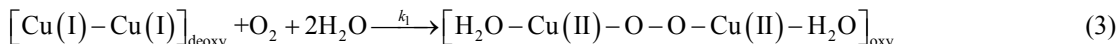
The system presented here is a cylindrical electrode which is uniformly coated by an enzyme immobilized in non-conducting material which is porous to substrate.

The electrode is used in a stirred solution containing an excess of supporting electrolyte. The enzyme and electrode reaction are [16]:

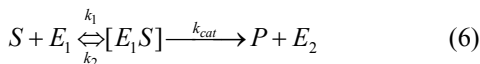


Hence the catechol/quinone conversion forms an am-

plification cycle within the enzyme film. While it is possible in principle to solve for either phenol or catechol as substrate, solving for catechol is simpler, since it involves only one enzymic conversion. The actual mechanism of that conversion is complex, and involves three different states, oxy, met, deoxy [17] *i.e.* (where Ca is catechol, Q is quinone).



It is assumed that the enzyme concentration is uniform and that the enzyme reaction follows Michaelis-Menten kinetics, in which case the reaction in the film is [18]



where

$$k_{cat} = k_1 c_{O_2} \quad \text{and} \quad K_M = \frac{k_1(k_2 + k_3)c_{O_2}}{k_2 k_3} \quad (7)$$

are the rate constant and Michaelis-Menten constant. The model of a cylindrical electrode modified with both an enzyme and conducting sites/particles (circles) is shown in **Figure 1**. The mass balance for catechol c_C can be written in cylindrical coordinates as follows:

$$\frac{D_C}{r} \frac{d}{dr} \left(r \frac{dc_C}{dr} \right) - \frac{k_{cat} c_E c_C}{c_C + K_M} = 0 \quad (8)$$

where c_C is the concentration profile of catechol, c_E is the concentration profile of enzyme, D_C and D_Q are its diffusion coefficients, and K_M is the Michaelis constant and c_Q is the concentration profile of quinone. Then the equation of continuum for quinone is generally expressed in the steady-state by [16]

$$\frac{D_Q}{r} \frac{d}{dr} \left(r \frac{dc_Q}{dr} \right) + \frac{k_{cat} c_E c_C}{c_C + K_M} = 0 \quad (9)$$

At the electrode surface (r_0) and at the film surface (r_1) the boundary conditions are given by [16]

$$\begin{aligned} r = r_0 : \quad c_C &= c_C^*, \quad c_Q = 0 \\ r = r_1 : \quad c_C &= c_C^*, \quad c_Q = 0 \end{aligned} \quad (10)$$

where c_C^* is the bulk concentration of catechol scaled by the partition coefficient of the enzyme film. Adding the **Eqs.8** and **9** and integrating with boundary condition (10), yields

$$\frac{c_C(r)}{c_C^*} + \frac{D_Q c_Q(r)}{D_C c_C^*} = 1 \quad (11)$$

The steady-state current can be given as [16]:

$$\frac{I}{nF} = 2\pi L r_0 D_Q \left(\frac{dc_Q}{dr} \right)_{r=r_0} \quad (12)$$

We introduce the following set of dimensionless variables:

$$\begin{aligned} C &= \frac{c_C}{c_C^*}, \quad Q = \frac{c_Q}{c_C^*}, \quad R = \frac{r}{r_0}, \quad \alpha = \frac{c_C^*}{K_M}, \quad \gamma_E = \frac{k_{cat} c_E r_0^2}{D_C K_M}, \\ \gamma_S &= \frac{k_{cat} c_E r_0^2}{D_Q K_M}, \quad \frac{D_Q}{D_C} = \frac{\gamma_E}{\gamma_S} \end{aligned} \quad (13)$$

where C and Q are the dimensionless concentration of the catechol and o -quinone. R is the dimensionless distance parameter. γ_E, γ_S and α are the dimensionless reaction-diffusion parameters and saturation parameter [16].

$$\frac{d^2 C}{dR^2} + \frac{1}{R} \frac{dC}{dR} - \frac{\gamma_E C}{1 + \alpha C} = 0 \quad (14)$$

$$\frac{d^2 Q}{dR^2} + \frac{1}{R} \frac{dQ}{dR} + \frac{\gamma_S C}{1 + \alpha C} = 0 \quad (15)$$

The boundary conditions are represented as follows:

$$C = 1, \quad Q = 0 \quad \text{when } R = 1 \quad (16)$$

$$C = 1, \quad Q = 0 \quad \text{when } R = r_1/r_0 \quad (17)$$

The dimensionless current at the micro-cylinder electrode can be given as follows:

$$\psi = I/nFL D_Q c_C^* = 2\pi (dQ/dR)_{R=1} \quad (18)$$

3. ANALYTICAL SOLUTIONS OF THE CONCENTRATIONS AND THE CURRENT USING THE HOMOTOPY PERTURBATION METHOD

Nonlinear phenomena play a crucial role in applied

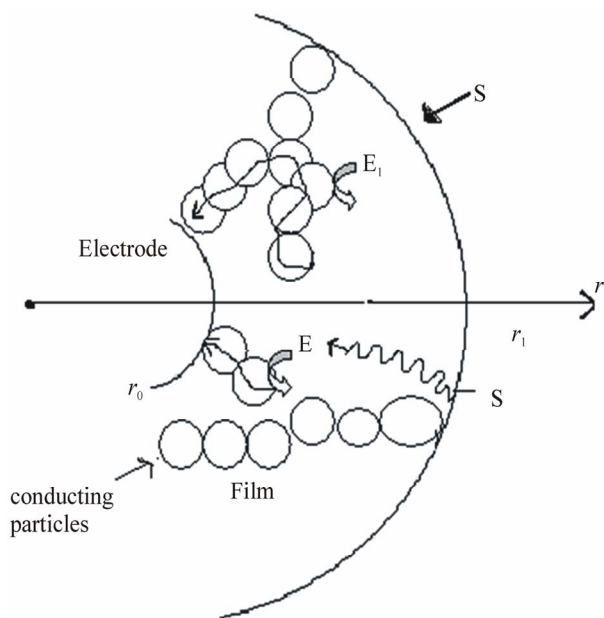


Figure 1. Illustration of the model of a cylindrical electrode modified with both an enzyme and conducting sites/particles (circles).

mathematics and chemistry. Construction of particular exact solutions for these equations remains an important problem. Finding exact solutions that have a physical, chemical or biological interpretation is of fundamental importance. This model is based on steady-state system of diffusion equations containing a non-linear reaction term related to Michaelis-Menten kinetics of the enzymatic reactions. It is not possible to solve these equations using standard analytical technique. In the past, many authors mainly had paid attention to study solution of nonlinear equations by using various methods, such as Backlund transformation [19], Darboux transformation [20], Inverse scattering method [21], Bilinear method [22], The tanh method [23], Variational iteration method [24] and Homotopy Perturbation Method [25-28] etc. The Homotopy Perturbation Method [25-28] has been extensively worked out over a number of years by numerous authors. The Homotopy Perturbation Method was first proposed by He [24-26] and was successfully applied to autonomous ordinary differential equations to nonlinear polycrystalline solids and other fields.

Recently Meena and Rajendran [29], Anitha *et al.* [30] and Manimozhi *et al.* [31] implemented Homotopy perturbation method to give approximate and analytical solutions of nonlinear reaction-diffusion equations con-

taining a nonlinear term related to Michaelis-Menten kinetic of the enzymatic reaction. Eswari *et al.* in series [32,33] solved the coupled non linear diffusion equations analytically for the microdisk and micro-cylinder enzyme electrode when a product from an immobilized enzyme reacts with the electrode. Using Homotopy Perturbation Method (see Appendix B), we can obtain the following solutions to the **Eqs.14 to 15**.

$$C(R) = 1 + \left[\frac{\gamma_E R^2 - \gamma_E (1 + r_1/r_0) R + \gamma_E (r_1/r_0)}{2(1 + \alpha)} \right] \quad (19)$$

$$Q(R) = \left[\frac{-\gamma_S R^2 + \gamma_S (1 + r_1/r_0) R - \gamma_S (r_1/r_0)}{2(1 + \alpha)} \right] \quad (20)$$

The **Eqs.19-20** satisfies the boundary conditions (16) to (17). These equations represent the new and simple analytical expression of the concentration of catechol and *o*-quinone for all possible values of the parameters γ_E , γ_S , α and r_1/r_0 . The **Eqs.19** and **20** also satisfy the relation

$C(R) + (\gamma_E/\gamma_S)Q(R) = 1$. From **Eqs.19** and **20**, we can obtain the dimensionless current, which is as follows:

$$\psi = I/nFLD_Q c_C^* = 2\pi \left[\frac{\gamma_S (1 + r_1/r_0) - 2\gamma_S}{2(1 + \alpha)} \right] \quad (21)$$

Eq. (21) represents the new and closed form of an analytical expression for the current for all possible values of parameters.

3.1. Limiting Cases for Unsaturated (First Order) Catalytic Kinetics

In this case, the catechol concentration c_C is less than Michaelis constant K_M . Now the **Eqs.8** and **9** reduce to the following forms:

$$\frac{D_C}{r} \frac{d}{dr} \left(r \frac{dc_C}{dr} \right) - \frac{k_{cat} c_E c_C}{K_M} = 0 \quad (22)$$

$$\frac{D_Q}{r} \frac{d}{dr} \left(r \frac{dc_Q}{dr} \right) + \frac{k_{cat} c_E c_C}{K_M} = 0 \quad (23)$$

By solving the **Eq.22** using the boundary condition (**Eq.10**), the concentration of catechol c_C can be obtained in the form of modified Bessel functions of zeroth order $I_0(\chi r)$ and $K_0(\chi r)$.

$$c_C(r)/c_C^* = \left[\frac{I_0(\chi r) [K_0(\chi r_0) - K_0(\chi r_1)] + K_0(\chi r) [I_0(\chi r_1) - I_0(\chi r_0)]}{K_0(\chi r_0) I_0(\chi r_1) - K_0(\chi r_1) I_0(\chi r_0)} \right] \quad (24)$$

where

$$\chi^2 = k_{cat} c_E / D_C K_M \quad (25)$$

Inserting **Eqs.24** into **Eqs.11**, we can obtain the concentration c_Q

$$\frac{D_Q c_Q(r)}{D_C c_C^*} = 1 - \left[\frac{I_0(\chi r) [K_0(\chi r_0) - K_0(\chi r_1)] + K_0(\chi r) [I_0(\chi r_1) - I_0(\chi r_0)]}{K_0(\chi r_0) I_0(\chi r_1) - K_0(\chi r_1) I_0(\chi r_0)} \right] \quad (26)$$

The sensor response j in terms of modified Bessel function of zeroth order can be obtained as follows:

$$j = \frac{I}{nFLD_C c_C^*} = \frac{2\pi\chi r_0}{[K_0(\chi r_0) I_0(\chi r_1) - K_0(\chi r_1) I_0(\chi r_0)]} \{K_1(\chi r_0) [I_0(\chi r_1) - I_0(\chi r_0)] - I_1(\chi r_0) [K_0(\chi r_0) - K_0(\chi r_1)]\} \quad (27)$$

4. COMPARISON WITH LIMITING CASE WORK OF RIJIRAVANICH *ET AL.* [16]

Recently, they [16] have derived the analytical expres-

sion of the steady- state concentration c_Q (**Eq.28** and sensor response j (**Eqs.28** and **29**) in integral form for the limiting case $c_C < K_M$.

$$\frac{D_Q c_Q(r)}{D_C c_C^*} = g\chi \left\{ -f \int_0^r I_1(\chi r) dr + \int_0^r K_1(\chi r) dr + \frac{\ln(r/r_0)}{\ln(r_1/r_0)} \left[f \int_0^{r_1} I_1(\chi r) dr - \int_0^{r_1} K_1(\chi r) dr \right] \right\} \quad (28)$$

$$j = \frac{I}{nFLD_C c_C^*} = 2\pi\chi g \times \left\{ r_0 [-f I_1(\chi r_0) + K_1(\chi r_0)] + \frac{1}{\ln(r_1/r_0)} \left[f \int_0^{r_1} I_1(\chi r) dr - \int_0^{r_1} K_1(\chi r) dr \right] \right\} \quad (29)$$

where

$$g = 1/[f I_0(\chi r_0) + K_0(\chi r_0)], \quad f = [K_0(\chi r_0) - K_0(\chi r_1)]/[I_0(\chi r_1) - I_0(\chi r_0)].$$

Rijiravanich *et al.* [16] obtained the empirical expression of the current

$$j = 2\pi x^q \tanh[(x/2)(\alpha_1 - 1)]^p \quad (30)$$

where p and q are empirical constants and $\alpha_1 = r_1/r_0$. The value of p and q are given for various values of $x (= \chi r_0)$ in the **Tables 1-3**. This empirical expression is compared our simple closed analytical expression **Eq.27**, in **Tables 2-3**. The average relative difference between our **Eq.27** and the empirical expression **Eq.30** is 0.71% when $\alpha_1 = 1.5$ and 0.59% when $\alpha_1 = 5$.

6. DISCUSSION

Figures 2 and **3** shows the dimensionless concentration profile of catechol $C(R)$ using **Eq.19** for all

Table 1. Values of p and q which fit **Eq.30** to **Eq.29** with < 5% error [16].

x	p	q
9.0-7.0	1.00	1.01
6.0-4.0	1.03	1.05
3.0	1.04	1.10
2.0	1.02	1.14 ^a /1.25 ^b

a Valid for $\alpha_1 \leq 2.0$; b Valid for $\alpha_1 > 2.0$

various values of the parameters γ_S , γ_E , r_1/r_0 and α . Thus it is concluded that there is a simultaneous increase in the values of the concentration of catechol as well as in saturated parameter α for small values of γ_E . Also the value of catechol concentration C is approximately equal to 1 when $R=1$ and $R=r_1/r_0$ for all values of α and γ_E .

Figures 4 and **5** show the concentration profile of *o*-quinone $Q(R)$ in R space for various values of α and γ_S calculated using **Eq.20**. The plot was constructed for $r_1/r_0 = 1.5$ and 5 . From these figures, it is confirmed that the value of the concentration of *o*-quinone increases when $\gamma_S \geq 0.1$ for small values of α . From the **Figures 2-5**, we can observed that the dimensionless concentration of catechol should vary between 0 and 1. Because catechol is converted to *o*-quinone, the *o*-quinone concentration should be the inverse of catechol. The substrate catechol C is minimum and product *o*-quinone Q is maximum when $R = (0.5 + r_1/2r_0)$ for all values of γ_S and α . The minimum value of concentration profile of catechol is

$$C_{\min} = \frac{8 + 8\alpha - \gamma_E + 2\gamma_E \alpha_1 - \gamma_E \alpha_1^2}{8(1 + \alpha)} \quad (31)$$

Table 2. Comparison of dimensionless sensor response j for various values of χr_0 using Eqs.27 and 30 when thickness of the film ($\alpha_1 = r_1/r_0 = 5$).

$x(= \chi r_0)$	$\alpha_1 = r_1/r_0$	p	q	Eq. (30) [16]	Eq. (27) This work	Error %
9	5	1	1.01	57.78	57.78	0.00
8	5	1	1.01	51.30	51.30	0.00
7	5	1	1.01	44.82	44.78	0.09
5	5	1.03	1.05	34.03	34.01	0.06
4	5	1.03	1.05	26.92	25.95	3.77
3	5	1.04	1.10	21.03	20.99	0.19
2	5	1.02	1.25	14.93	14.93	0.01
Average % deviation						0.59

Table 3. Comparison of dimensionless sensor response j for various values of χr_0 using Eqs.27 and 30 when thickness of the film ($\alpha_1 = r_1/r_0 = 1.5$).

$x(= \chi r_0)$	$\alpha_1 = r_1/r_0$	p	q	Eq. (30) [16]	Eq. (27) This work	Error %
9	1.5	1	1.01	56.51	56.51	0.00
8	1.5	1	1.01	49.45	49.45	0.01
7	1.5	1	1.01	42.20	42.19	0.02
5	1.5	1.03	1.05	28.62	27.60	3.67
4	1.5	1.03	1.05	20.27	20.43	0.80
3	1.5	1.04	1.10	13.09	13.15	0.45
2	1.5	1.02	1.14	6.32	6.32	0.01
Average % deviation						0.71

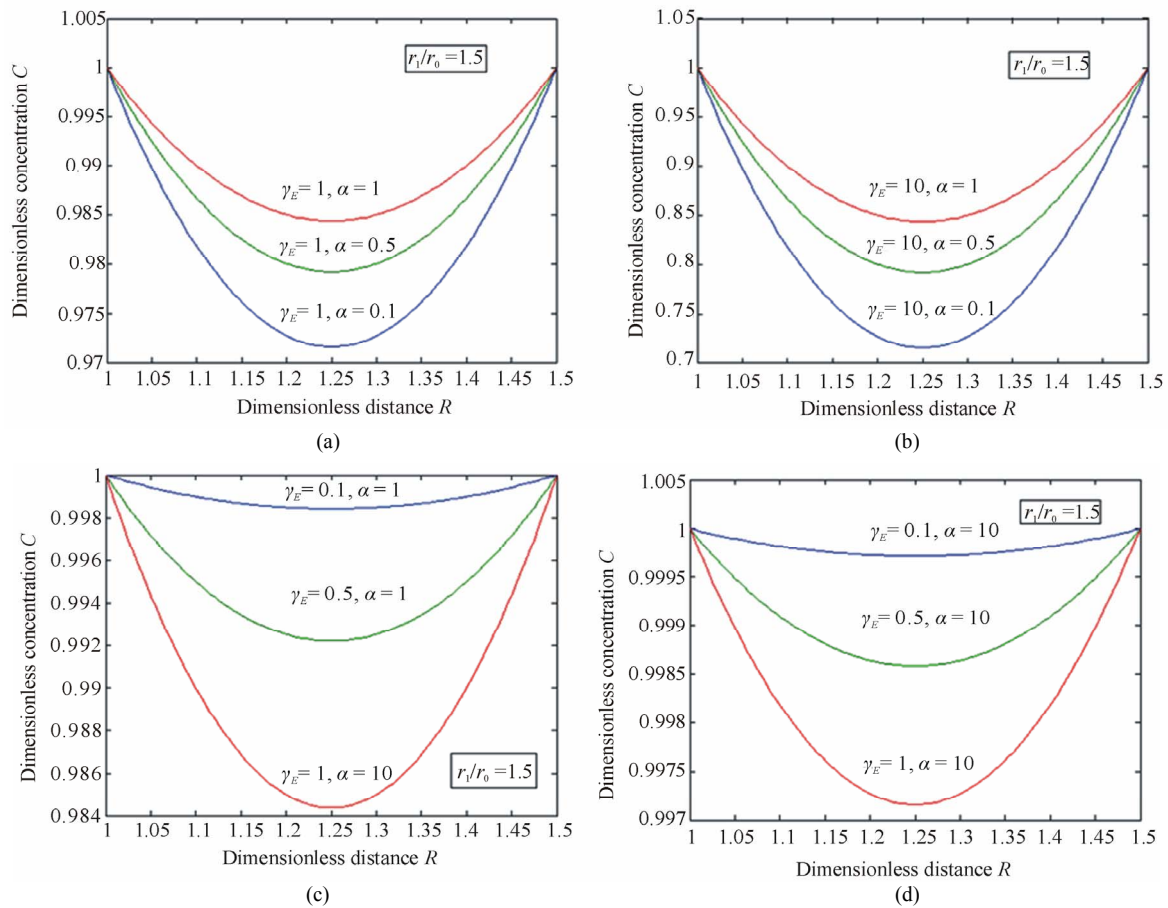


Figure 2. Typical normalized steady-state concentration profile of catechol $C(R)$ plotted from Eq.19 for different values of parameters γ_E and α when $r_1/r_0 = 1.5$.

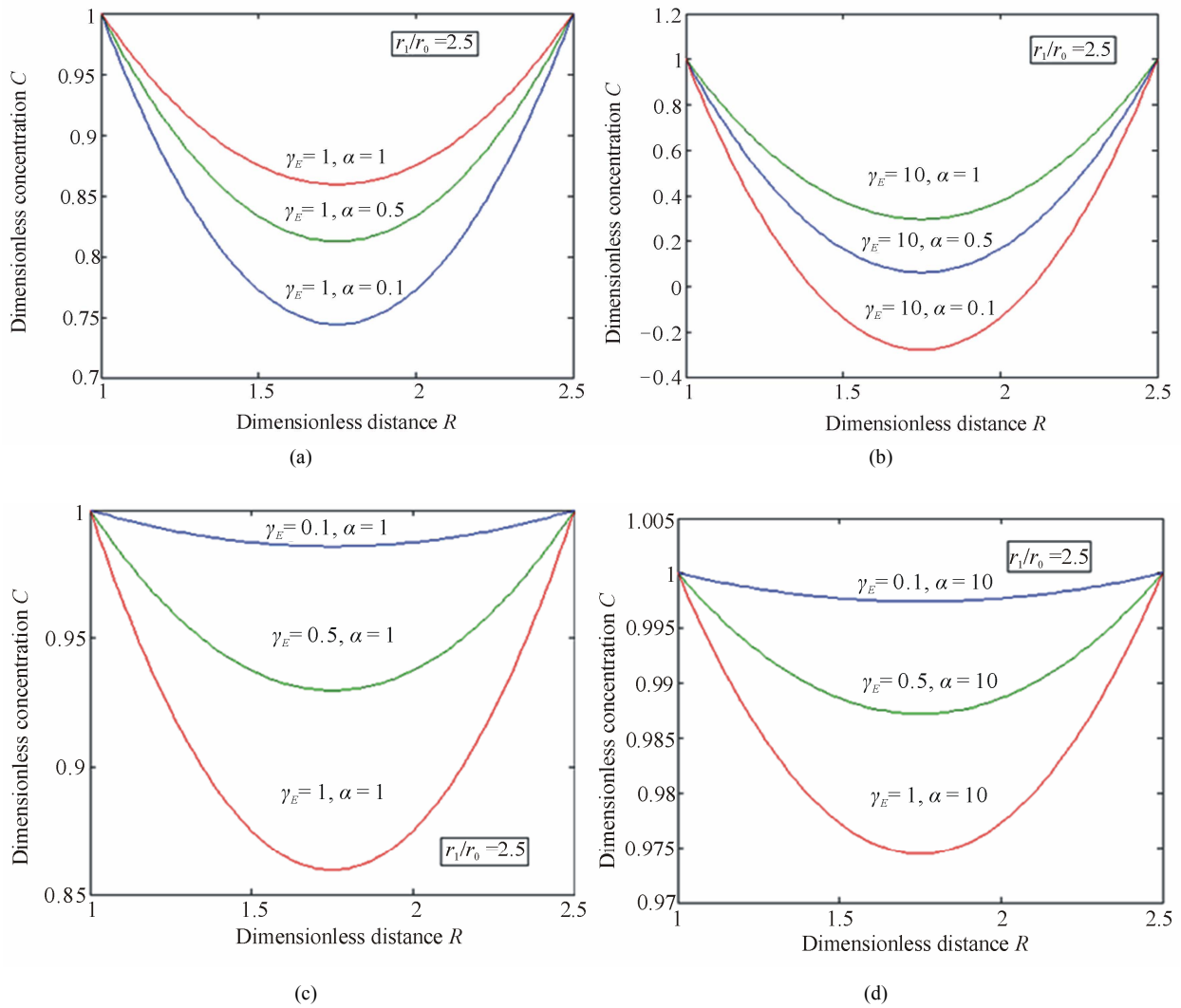
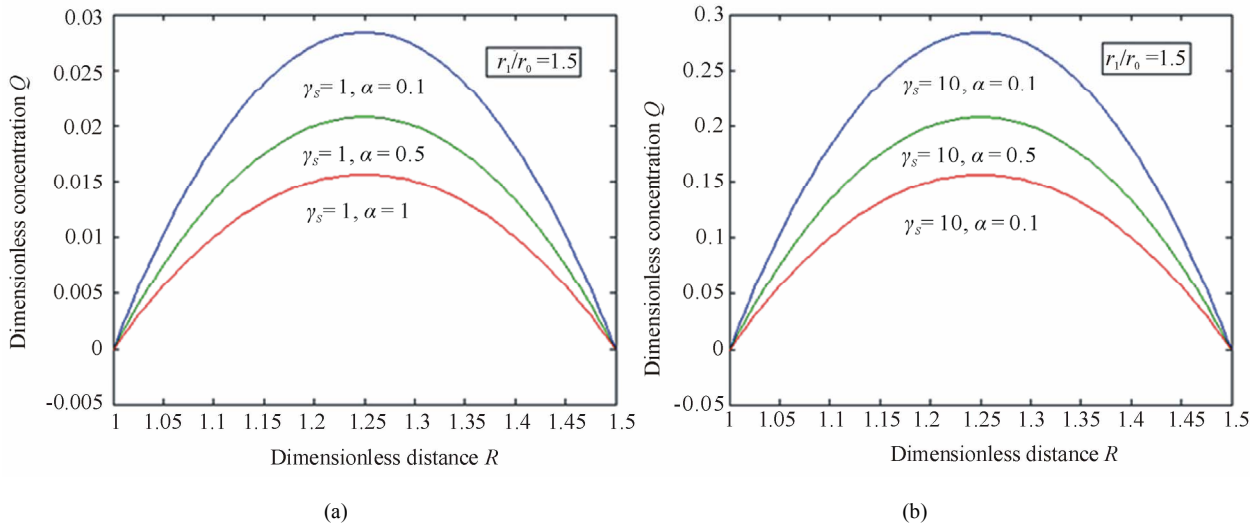


Figure 3. Typical normalized steady-state concentration profile of $C(R)$ plotted from Eq. 19 for different values of parameters γ_E and α when $r_1/r_0 = 2.5$.



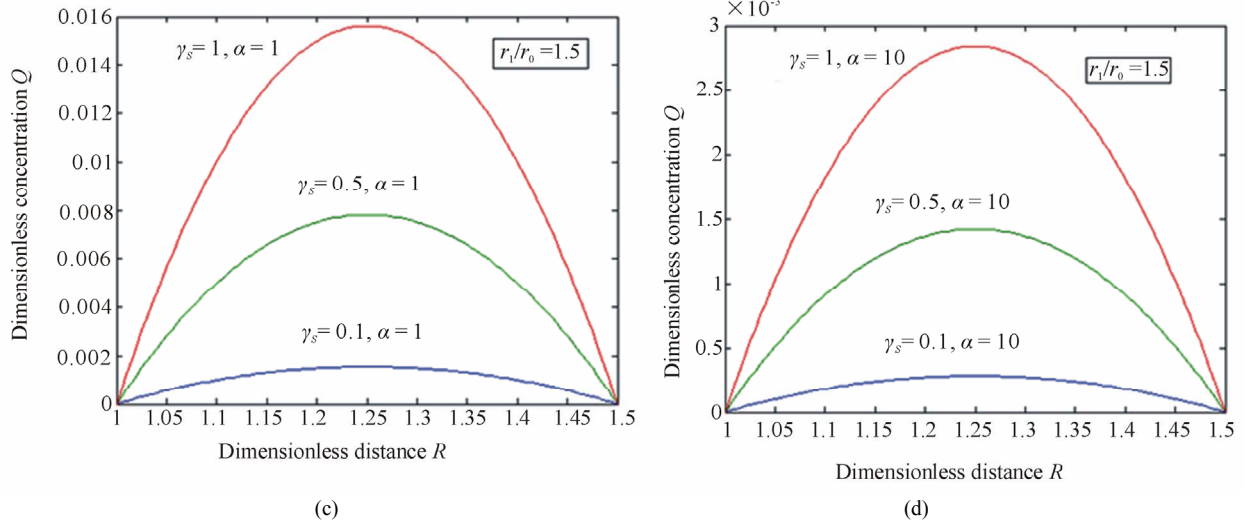


Figure 4. Typical normalized steady-state concentration profile of $Q(R)$ plotted from **Eq.20** for different values of parameters γ_E and α when $r_1/r_0 = 1.5$.

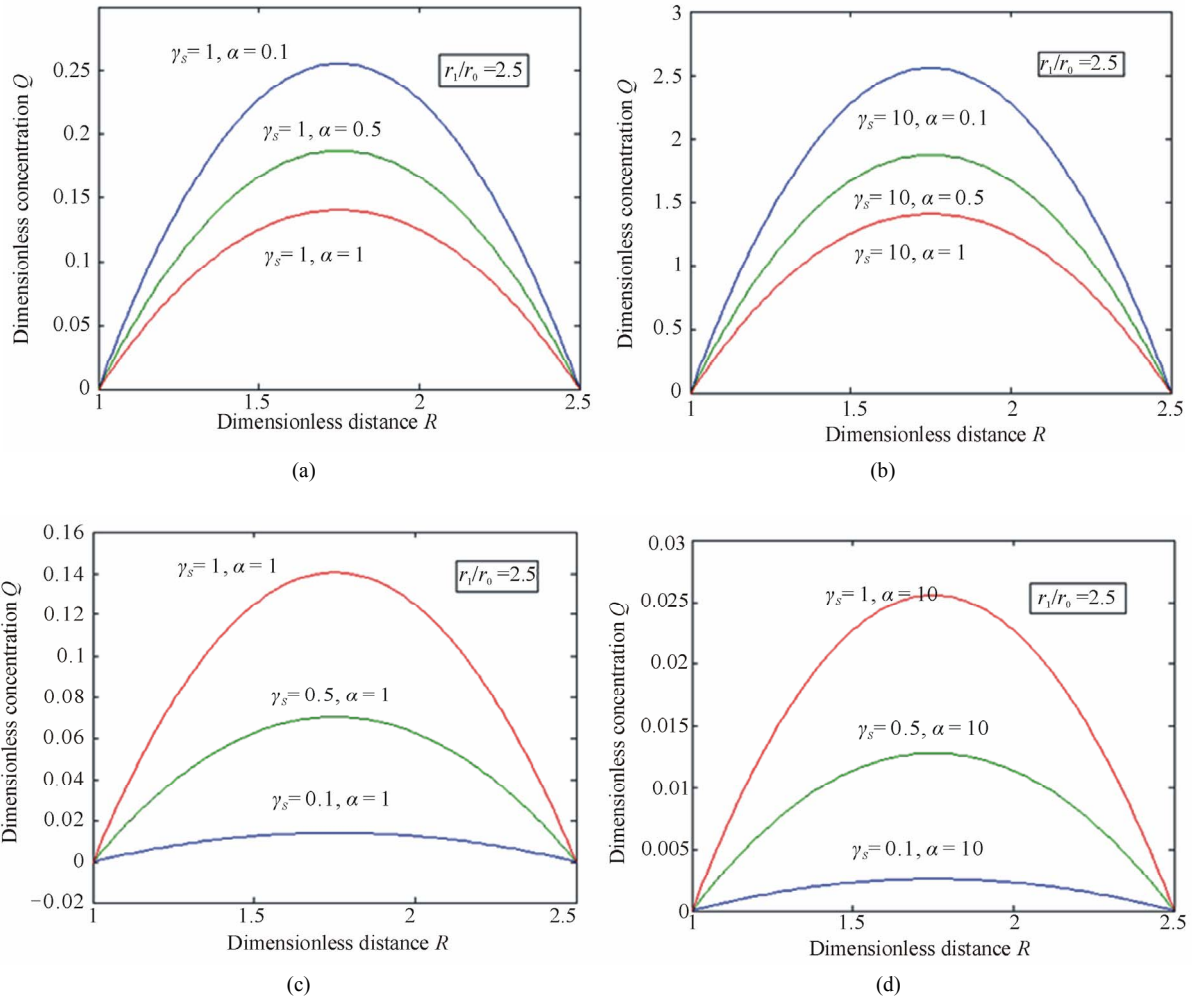


Figure 5. Typical normalized steady-state concentration profile of $Q(R)$ plotted from **Eq.20** for different values of parameters γ_E and α when $r_1/r_0 = 2.5$.

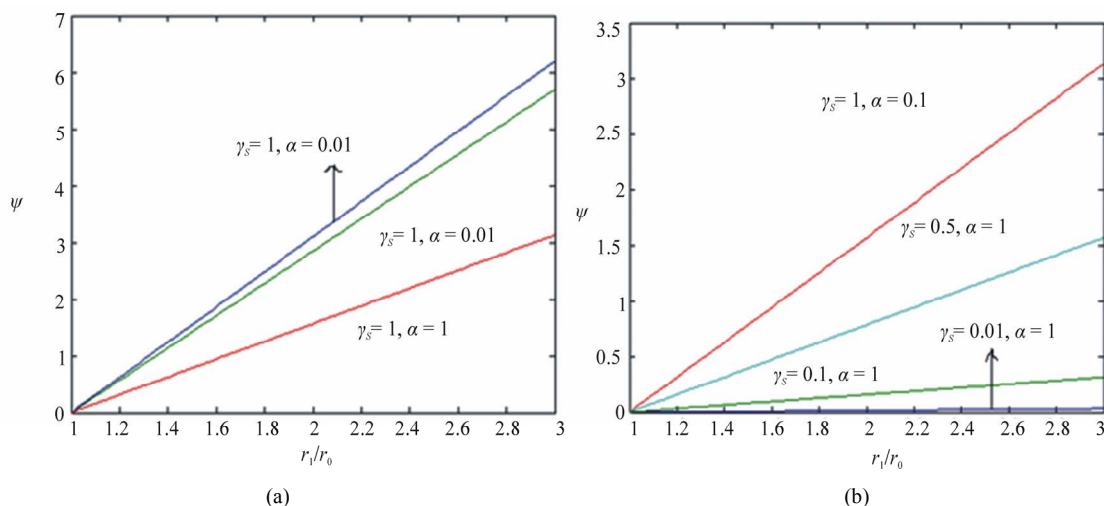


Figure 6. Plot of dimensionless current ψ versus r_1/r_0 . Current is calculated in the Eq.21.

and the maximum value of concentration profile of quinone is

$$Q_{\max} = \frac{\gamma_s(1-2\alpha_1 + \alpha_1^2)}{8(1+\alpha)} \quad (32)$$

where $r_1/r_0 = \alpha_1$. The dimensionless current ψ versus r_1/r_0 using Eq.21 is plotted in Figure 6. The value of current ψ increases when thickness of the film r_1/r_0 and dimensionless reaction-diffusion parameter γ_s is increases or decreases.

7. CONCLUSIONS

A non-linear time independent ordinary differential equation has been formulated and solved analytically. Analytical expression for the concentration of catechol and *o*-quinone and steady state current are derived by contains significant non-linear contributions using the Homotopy Perturbation Method. The primary result of this work is simple approximate calculation of concentration of catechol, *o*-quinone and current for all values of γ_E , γ_S , α and r_1/r_0 and χr_0 . Formerly in polyphenol oxidase micro-cylinder biosensor models are [16] have only considered the first order kinetics of the enzyme and therefore could only be applied to the sensor's linear range. However, in this paper, calibration curves of many of the catechol/phenol biosensors contain most important non-linear contributions are reported. Also, the length of the linear range is an important analytical parameter. In developing a sensor, experimental scientists would like this range to cover all concentrations expected in actual samples, as this makes calibration of the sensor in the field much easier. In Tables 2-3, our analytical results are compared with limiting case of first order catalytic kinetics [16] results, which yield a good agreement with the previous limiting case results.

8. ACKNOWLEDGEMENTS

This work was supported by the Council of Scientific and Industrial Research (CSIR No.: 01(2442)/10/EMR-II), Government of India. The authors also thank Mr. M. S. Meenakshisundaram, Secretary, The Madura College Board, Dr. R. Murali, The Principal, and S. Thia-garajan, Head of the Department, Madura College, Madurai, India for their constant encouragement. The authors K. Venugopal and A. Eswari are very thankful to the Manonmaniam Sundaranar University, Tirunelveli for allowing to do the research work.

REFERENCES

- [1] Revzin, A.F., Sirkar, K., Simonian, A. and Pishko, M.V. (2002) Glucose, lactate and pyruvate biosensor arrays based on redox polymer/oxidoreductase nanocomposite thin films deposited on photolithographically patterned gold electrodes. *Sensor and Actuators B*, **81**, 359. doi:10.1016/S0925-4005(01)00982-0
- [2] Shi, G., Liu, M., Zhu, M., Zhou, T., Chen, J., Jin, L. and Jin, J.-Y. (2002) The study of nafion/xanthine oxidase/au colloid chemically modified biosensor and its application in the determination of hypoxanthine in myocardial cells in vivo. *Analyst*, **127**, 396. doi:10.1039/b108462n
- [3] Gue, A.-M., Tap, H., Gros, P. and Maury, F. (2002) A miniaturized silicon based enzymatic biosensor: Towards a generic structure and technology for multi-analytes assays. *Sensor and Actuators B*, **82**, 227. doi:10.1016/S0925-4005(01)01009-7
- [4] Edmonds, T.E. (1985) Electroanalytical application of carbon fiber electrodes, *Analytica Chimica Acta*, **175**, 1. doi:10.1016/S0003-2670(00)82713-0
- [5] Gonon, F., Suaud-Changny, M.F. and Buda, M. (1992) Proceedings of satellite symposium on neuro-science and technology, Lyon, 215.
- [6] Donnet, J.B. and Basal, R.C. (1984) International Fiber Science and Technology, Carbon Fibers, Dekker, New York, **3**.

- [7] Decher, G. and Hong, J.D. (1991) Buildup of ultrathin multilayer films by a self-assembly process: II. Consecutive adsorption of anionic and cationic bipolar amphiphiles and polyelectrolytes on charged surfaces. *Berichte der Bunsengesellschaft Für Physikalische Chemie*, **95**, 1430.
- [8] Hodak, J., Etchenique, R., Calvo, E.J., Singhal, K. and Bartlett, P.N. (1997) Layer by layer self assembly of glucose oxidase with a poly(allylamine)-ferrocene redox mediator. *Langmuir*, **13**, 2708. doi:10.1021/la962014h
- [9] Forzani, E.S., Solis, V.M. and Calvo, E.S. (2000) Electrochemical behavior of polyphenol oxidase immobilized in self-assembled structures layer by layer with cationic polyallylamine. *Analytical Chemistry*, **72**, 5300. doi:10.1021/ac0003798
- [10] Coche-Guerante, L., Labbe, P. and Mengeand, V. (2001) *Analytical Chemistry*, **73**, 3206. doi:10.1021/ac001534i
- [11] Lvov, Y. and Caruso, F. (2001) Biocolloids with ordered urease multilayer shells as enzymatic reactors. *Analytical Chemistry*, **73**, 4212. doi:10.1021/ac010118d
- [12] Fang, M., Grant, P.S., McShane, M.J., Sukhorukov, G. B., Golub, V.O. and Lvov, Y. (2002) Magnetic bio/nanoreactor with multilayer shells of glucose oxidase and inorganic nanoparticles. *Langmuir*, **18**, 6338. doi:10.1021/la025731m
- [13] Caruso, F. and Schuler, C. (2000) Enzyme multilayers on colloid particles: Assembly, stability, and enzymatic activity. *Langmuir*, **16**, 9595. doi:10.1021/la000942h
- [14] Caruso, F., Fiedler, H. and Haage, K. (2000) Assembly of β -glucosidase multilayers on spherical colloidal particles and their use as active catalyst. *Colloids and Surfaces A: Physicochemical and Engineering Aspects*, **169**, 287. doi:10.1016/S0927-7757(00)00443-X
- [15] Sun, H. and Hu, N. (2004) I. Voltammetric studies of hemoglobin-coated polystyrene latex bead films on pyrolytic graphite electrodes. *Biophysical Chemistry*, **110**, 297. doi:10.1016/j.bpc.2004.03.005
- [16] Rijiravanich, P., Aoki, K. and Chen, J., Surareungchai, W. and Somasundrum, M. (2006) Micro-cylinder biosensors for phenol and catechol based on layer-by-layer immobilization of tyrosinase on latex particles: Theory and experiment. *Journal of Electroanalytical Chemistry*, **589**, 249-258. doi:10.1016/j.jelechem.2006.02.019
- [17] Wilcox, D.E., Porras, A.G., Hwang, Y.T., Lerch, K., Winkler, M.E. and Solomon, E.I. (1985) Substrate Analogue Binding to the Coupled Binuclear Copper Active Site in Tyrosinase. *Journal of American Chemical Society*, **107**, 4015. doi:10.1021/ja00299a043
- [18] Carbanes, J., Garcia-Canovas, F., Lozano, J.A. and Garcia-Carmona, F. (1987) A kinetic study of the melanization pathway between L-tyrosine and dopachrome. *Biochimica et Biophysica Acta-General Subjects*, **923**, 187.
- [19] Coely, A., *et al.* (2001) Backlund and darboux transformation. American Mathematical Society, Providence, RI.
- [20] Wadati, M., Sanuki, H. and Konno, K. (1975) Relationships among inverse method, backlund transformation and an infinite number of conservation laws. *Progress of Theoretical Physics*, **53**, 419. doi:10.1143/PTP.53.419
- [21] Gardener, C.S., Green, J.M., Kruskal, M.D. and Miura, R.M. (1967) Method for solving the Korteweg-de Vries equation. *Physical Review Letter*, **19**, 1095. doi:10.1103/PhysRevLett.19.1095
- [22] Hirota, R. (1971) Exact solutions to the equation. describing cylindrical solitons. *Physical Review Letter*, **27**, 1192. doi:10.1103/PhysRevLett.27.1192
- [23] Malfliet, W. (1992) Solitary wave solutions of nonlinear wave equations. *American Journal of Physics*, **60**, 650. doi:10.1119/1.17120
- [24] He, J.H. (1998) Approximate analytical solution for seepage flow with fractional derivatives in porous media. *Computer Methods in Applied Mechanics and Engineering*, **167**, 57. doi:10.1016/S0045-7825(98)00108-X
- [25] He, J.H. (2005) Approximate solution of nonlinear differential equations with convolution product nonlinearities. *Computer Methods in Applied Mechanics and Engineering*, **26**, 695-700.
- [26] He, J.H. (2006) Homotopy perturbation method for solving boundary value problems. *Physical Letter A*, **350**, 87-88. doi:10.1016/j.physleta.2005.10.005
- [27] Ariel, P.D. (2010) Homotopy perturbation method and the natural convection flow of a third grade fluid through a circular tube. *Nonlinear Science Letters A*, **1**, 43-52.
- [28] Ganji, D.D. and Rafei, M. (2006) Solitary wave solutions for a generalized Hirota-satsuma coupled KdV equation by homotopy perturbation Method. *Physical Letter A*, **356**, 131-137. doi:10.1016/j.physleta.2006.03.039
- [29] Meena, A. and Rajendran, L. (2010) Mathematical modeling of amperometric and potentiometric biosensors and system of non-linear equations-Homotopy perturbation approach. *Journal of Electroanalytical Chemistry*, **644**, 50-59. doi:10.1016/j.jelechem.2010.03.027
- [30] Anitha, S., Subbiah, A., Rajendran, L. and Ashok K.J. (2010) Solutions of the coupled reaction and diffusion equations within polymer-modified ultramicroelectrodes. *Physical Chemistry C*, **114**, 7030-7037.
- [31] Manimozhi, P., Subbiah, A. and Rajendran, L. (2010) Solution of steady-state substrate concentration in the action of biosensor response at mixed enzyme kinetics. *Sensor and Actuators B*, **147**, 290-297. doi:10.1016/j.snb.2010.03.008
- [32] Eswari, A. and Rajendran, L. (2010) Analytical solution of steady state current at a microdisk biosensor. *Journal of Electroanalytical Chemistry*, **641**, 35-44. doi:10.1016/j.jelechem.2010.01.015
- [33] Eswari, A. and Rajendran, L. (2010) Analytical solution of steady-state current an enzyme-modified microcylinder electrodes. *Journal of Electroanalytical Chemistry*, **648**, 36-46. doi:10.1016/j.jelechem.2010.07.002

APPENDIX A SYMBOLS USED

Symbol	Definitions	Units
D_C	Diffusion coefficient of catechol	cm ² /s
c_C	Concentration profile of catechol	mole/cm ³
c_E	Concentration profile of enzyme	mole/cm ³
K_M	Michaelis Menten constant	mole/cm ³
K_{cat}	Catalytic rate constant	sec ⁻¹
c_Q	Concentration profile of quinone	mole/cm ³
D_Q	Diffusion coefficient of quinone	cm ² /s
c_C^*	Bulk concentration of C	mole/cm ³
r	Radius of the cylinder	cm
I	Current	ampere
r_0	Electrode radius	cm
r_1	Film radius	cm
r_1/r_0	Dimensionless parameter for film thickness	none
χr_0	Dimensionless parameter for enzyme kinetic	none
j	Dimensionless sensor response	none
ψ	Dimensionless current	none
C	Dimensionless concentration of catechol	none
Q	Dimensionless concentration of quinone	none
R	Dimensionless distance	none
γ_E	Dimensionless reaction diffusion parameter	none
γ_S	Dimensionless reaction diffusion parameter	none
α	Dimensionless saturation parameter	none
L	Length of the electrode	cm
F	Faraday constant	c·mole ⁻¹
n	Number of electrons	none

APPENDIX B

Solution of the **Eqs.14** and **15** using Homotopy perturbation method. In this appendix, we indicate how **Eqs.19** and **20** in this paper are derived. Furthermore, a Homotopy was constructed to determine the solution of **Eqs.14** and **15**.

$$(1-p) \left[\frac{d^2 C}{dR^2} \right] + p \left[\frac{d^2 C}{dR^2} + \frac{1}{R} \frac{dC}{dR} - \frac{\gamma_E C}{1+\alpha C} \right] = 0 \quad (\text{B1})$$

$$(1-p) \left[\frac{d^2 Q}{dR^2} \right] + p \left[\frac{d^2 Q}{dR^2} + \frac{1}{R} \frac{dQ}{dR} + \frac{\gamma_S C}{1+\alpha C} \right] = 0 \quad (\text{B2})$$

and the initial approximations are as follows:

$$R=0, C=1, Q=0 \quad (\text{B3})$$

$$R = \frac{r_1}{r_0}, C=1, Q=0 \quad (\text{B4})$$

The approximate solutions of **(B1)** and **(B2)** are

$$C = C_0 + pC_1 + p^2C_2 + p^3C_3 + \dots \quad (\text{B5})$$

and

$$Q = Q_0 + pQ_1 + p^2Q_2 + p^3Q_3 + \dots \quad (\text{B6})$$

Substituting **Eqs.B5** and **B6** into **Eqs.B1** and **B2** and comparing the coefficients of like powers of p

$$p^0 : \frac{d^2C_0}{dR^2} = 0 \quad (\text{B7})$$

$$p^1 : \frac{d^2C_1}{dR^2} + \frac{1}{R} \frac{dC_0}{dR} - \frac{\gamma_E C_0}{1 + \alpha C_0} = 0 \quad (\text{B8})$$

and

$$p^0 : \frac{d^2Q_0}{dR^2} = 0 \quad (\text{B9})$$

$$p^1 : \frac{d^2Q_1}{dR^2} + \frac{1}{R} \frac{dQ_0}{dR} + \frac{\gamma_S C_0}{1 + \alpha C_0} = 0 \quad (\text{B10})$$

Solving the **Eqs.B7** to **B10**, and using the boundary conditions **(B3)** and **(B4)**, we can find the following results

$$C_0(R) = 1 \quad (\text{B11})$$

$$C_1(R) = \frac{\gamma_E R^2 + \gamma_E (r_1/r_0) - \gamma_E (1 + r_1/r_0)R}{2(1 + \alpha)} \quad (\text{B12})$$

and

$$Q_0(R) = 0 \quad (\text{B13})$$

$$Q_1(R) = \frac{\gamma_S (1 + r_1/r_0)R - \gamma_S (r_1/r_0) - \gamma_S R^2}{2(1 + \alpha)} \quad (\text{B14})$$

According to the HPM, we can conclude that

$$C(R) = \lim_{p \rightarrow 1} C(R) = C_0 + C_1 + C_2 + \dots \quad (\text{B15})$$

$$Q(R) = \lim_{p \rightarrow 1} Q(R) = Q_0 + Q_1 + Q_2 + \dots \quad (\text{B16})$$

Using **Eqs.B11** and (B12) in **Eq.B15** and **Eqs.B13** and **B14** in **Eq.B16**, we obtain the final results as described in **Eqs.19** and **20**.